Building Tomorrow's Society

Bâtir la Société de Demain

Fredericton, Canada

June 13 – June 16, 2018/ *Juin 13 – Juin 16, 2018*

THE USE OF DIGITAL IMAGE CORRELATION TO DEMONSTRATE TENSION MEMBER BEHAVIOUR IN STRUCTURAL STEEL DESIGN

McNeill, Nathan[1], Lloyd, Alan[1,2]
[1] Department of Civil Engineering, University of New Brunswick, Canada
[2] alan.lloyd@unb.ca

Abstract: When first introducing students to structural steel, the design of tension members can be a difficult concept to understand. For bolted tension members, an analogy can be made to the capacity being the weakest link in a chain. For the design of bolted tension members, many potential ultimate limit states must be considered including yielding, fracture in tension, shear and tension block failure, inclined tension failure in the case of staggered bolts, shear lag, bolt bearing, and bolt shear. The different nature and high number of these potential failure modes make learning the design of tension members a considerable challenge for new students. A testing program was conducted at the University of New Brunswick to explore the different failure mechanisms of tension members with a goal of creating qualitative and quantitative content to incorporate into teaching of undergraduate civil engineering students. Digital image correlation (DIC) was used to monitor the tests and compute shear and tension strain fields that provide visual and numerical validation of design concepts. Presented in this paper are the results from the testing of three different structural members: a flat bar, an angle, and a channel.

1 INTRODUCTION

The design of tension members can be a difficult concept for students to grasp when seeing it for the first time. This is due to the high number of failure modes and the significant differences between them. When looking at a bolted connection, there are numerous ultimate limit states that could lead to the eventual failure of a member.

To help students better understand how certain failure modes occur, several structural steel members were tested in tension up to failure. Included in these members were plates, channels, and angles all with different bolt configurations. For this paper, three members were chosen to analyze: a flat bar (FB6.1X152) with a staggered bolt pattern, an angle (L102X102X9.5) with two lines of transverse bolts, and, a channel (C150X12) with three transverse lines of bolts. The connections for each of these members were designed to show a different failure mode. The staggered bolt pattern on the flat bar was to show an inclined tension plane fracture, and the transverse bolts on the angle and channel were to show a tension and shear block failure, as well as shear lag on the outstanding components of the connection. All testing was completed on a universal testing machine (UTM) using adaptable mounting plates to bolt the specimens to the UTM, such that the applied tension force was concentric through the middle of the bolt groups. The test setup is shown in Figure 1.

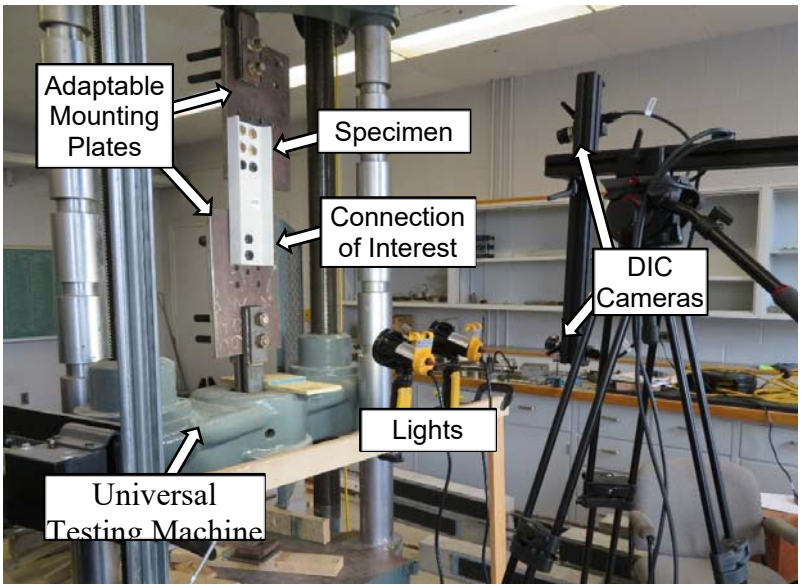

Figure 1: Test configuration

Digital image correlation (DIC) was used to help visualize the tension and shear strains that are introduced into each member. DIC is an optical, non-contact measurement technique used for measuring displacements-based quantities including continuous strain fields in experimental research (McCormick and Lord 2010). When compared with conventional methods of gathering strain and displacement information such as, strain gauges, linear variable displacement transducers, and extensometers, DIC can gather more information in much greater detail. DIC tracks the deformation in a speckle pattern on a high contrast surface. In this case, the steel specimens were painted white and a black speckle pattern was applied using spray paint. Using DIC software, 3D plots of the strain fields that are induced in the member under load can be defined and presented in a very simple and effective way. The two camera DIC monitoring setup is shown in Figure 1.

The DIC software, in conjunction with a universal testing machine, were used to validate the S16 design equations for structural steel in tension and give a real-life demonstration of the behaviour of structural steel. These results are being developed into teaching aids for use in university structural steel design courses.

2 EXPERIMENTAL PROGRAM

All three members presented in this paper were connected using bolt groups. All bolts used were ¾" (19mm diameter) SAE Grade 8 bolts. The SAE bolts were selected over ASTM A490 bolts due to their smaller head sizes than the heavy-hex structural bolts. The ultimate strengths of the Grade 8 bolts are specified as 1035MPa (SAE 2011), the same as ASTM A490 bolts (ASTM 2015). Unlike ASTM bolts, the threads on SAE bolts extend the entire bolt length meaning that all connections had shear planes intercepting threads of bolts and bolts always bared on the base material over a threaded length. All bolt holes for all connections were drilled to 13/16" (20.6mm) diameter using an annular cutter drill bit.

The first connection that was tested was a plate (FB6.1X152) with four ¾" bolts in a staggered pattern. Figure 2a shows the details of the tension member and connection, while Figure 2b shows the actual specimen prior to testing. In Figure 2b, the two sides of the specimen can be seen to have different connection detailing. This is typical of all specimens tested for this study. Specimens were designed to have significantly different capacity at either end. The first test on a specimen would cause failure in the lower capacity connection. After that test, the failed side of the specimen was welded to a new mounting plate and the tension test was conducted again to fail the other side of the specimen, which would now have the lowest capacity vs the new welded connection. Figure 2c shows the area of interest for this test, the

staggered connection. This image is taken from one of the DIC cameras. Here, the applied speckle pattern of black paint on a white painted surface that is used for the DIC measurements is shown. Also shown are the bolt heads which were painted flat black to reduce reflections and glare.

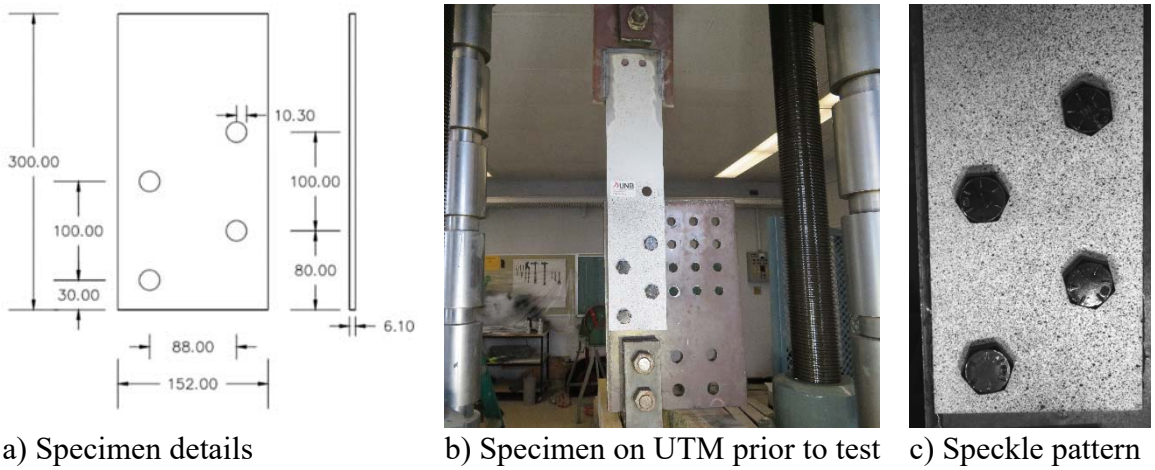

a) Specimen details b) Specimen on UTM prior to test c) Speckle pattern

Figure 2: Details of staggered bolted FB6.1X152 connection prior to testing

The channel (C150X12) was designed with six ¾" bolts in three transverse lines of two bolts as shown in Figure 3. This bolt pattern was picked to promote a shear block failure. In addition to using the DIC monitoring to explore the tension and shear block failure for this connection, the cameras were placed slightly skewed to the plane of the channel web in order to keep one flange visible during testing as shown in Figure 3c. This was done to allow the DIC system to monitor shear lag in the outstanding components of the connection in order to show the non-uniform strain fields in such connections. Even though the ultimate failure mode for this connection is a shear block, shear lag is present in the connection leading up to failure and becomes demonstrable with the DIC visualizations presented later in this paper.

a) Specimen details b) Specimen on UTM prior to test c) Speckle pattern

Figure 3: Details of bolted C150X12 connection prior to testing

The angle (L102X102X9.5) was designed with two transverse lines of two bolts (a four-bolt group) as shown in Figure 4. Note that Figure 4b shows the specimen after failure due to a lack of pre-test photos for this specimen. The angle was designed to fail in a shear block with the free edge of the connected leg rupturing in tension, and then a shear plane failure along the two bolts closest to the outstanding leg continuing to the end of the tension member. Since only one leg of the angle is connected, this test was also designed to show the effects of shear lag on the outstanding leg of the angle. Once again, like for the channel, the cameras were placed on skewed angle to the plane of the bolted leg to clearly see the outstanding leg and

measure the shear lag effects. This can be seen in Figure 4c, where the view of one of the DIC cameras is presented showing the measurement area and the speckle pattern that was applied to the specimen prior to testing.

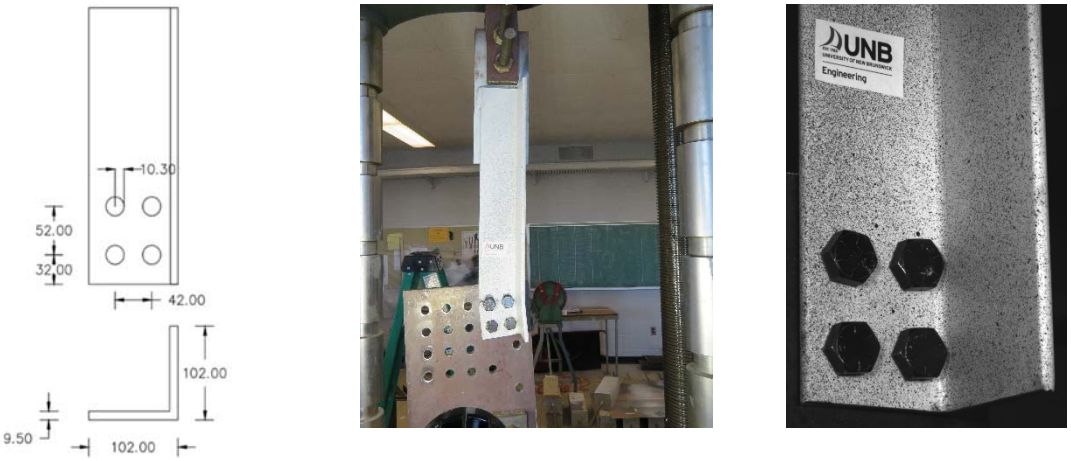

a) Specimen details b) Specimen on UTM after the test c) Speckle pattern

Figure 4: Details of bolted L102x102x9.5 connection prior to testing

2 EXPERIMENTAL RESULTS

Dog bone coupons were cut from the material of each member and in a universal testing machine to determine material tension properties. The coupons were tested with a constant displacement rate of 2mm/minute. Force was recorded from a data logger monitoring a load cell on the UTM and elongation was measured using DIC. Figure 5 shows the stress-strain response of the three materials tested here. As shown, the material behaviour for the angle and channel is representative of structural steel with a clearly defined yield point followed by a plastic plateau leading into strain hardening, necking, and rupture. The coupon cut from the flat bar did not have a clearly defined yield point and the yield and ultimate stresses were nearly the same. The measured material strengths for yield (F_y) and ultimate (F_u) stress are provided inset in Figure 5. The coupon shown in Figure 5 has the DIC measured longitudinal strain field at the onset of necking overlaid on its surface. The necking point can be identified by the concentrations of high strains.

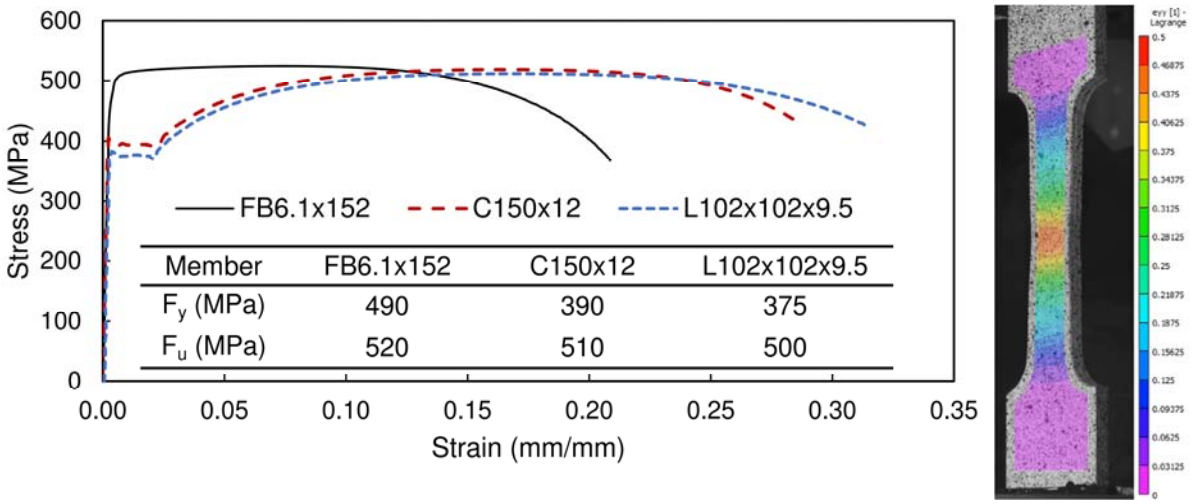

Figure 5: Stress strains curves for the three specimens along with DIC strain field on coupon

The force-time histories for the three specimen tests are shown in Figure 6. Since the UTM loaded the specimens under a constant displacement rate of 5mm/minute, the cross-head displacement is proportional to the time axis. All specimens show an initial soft response in early times as the test coupling systems seat themselves into the UTM. During this time, the material is behaving linearly, although the force-time or a force-displacement curve shows a non-linear response due to support seating. Following the initial soft response, the specimens behaved elastically, with force increasing linearly with time (proportional to displacement). The flat bar with staggered bolts showed an extended period of plastic displacement, when force was not increasing with cross-head movement. This plasticity correlates to the yielding and strain hardening of the tension failure plane that formed between the edges of the plate, and the bolt holes and the inclined failure surface that formed between the two leading staggered bolts. The inset failed specimen image clearly shows this failure plane. Fracture of this specimen initiated in the edges between the holes and the plate edges. Once this fracture occurred, the tension capacity of the plate rapidly dropped, and the inclined fracture occurred which completely severed the tension member.

The C150x12 member failed in a tension and shear block mode as shown in the inset failure image in Figure 6. At around 230 seconds, after the start of the test, the first fracture of the connection occurred. This is shown by a sudden decrease in the tension load on the force-time history. The first fracture for this connection was a shear fracture in the regions between the trailing bolts (final transverse line of bolts) and the end of the channel web. After this, the specimen continued to hold load until around 260 seconds where a second fracture failure occurs. This second fracture was a tension failure between the two leading bolts. Once this occurred, the force capacity of the member dropped suddenly, and the specimen continued to be displaced until the complete fracture of the tension and shear block occurred, with the remaining shear fractures along the edges of the bolts.

The L102x102x9.5 specimen also failed in a tension and shear block mode. The first component of this failure occurred at approximately 230 seconds where a tension fracture plane formed between one of the leading bolts and the free edge of the connected leg. Following the corresponding drop in force with the first fracture, the specimen was able to hold a reduced load for a short duration of testing time until the next tension fracture occurred at about 240 seconds. This fracture was a pure tension failure of the plane between the two leading bolts in the connection. The inset image of the failed specimen shows these fractures. Once the tension fractures had occurred, the force capacity of the specimen was greatly reduced and the test was terminated. It was not possible to cause a shear fracture that would have completely removed the tension and shear block in this specimen due to the large eccentricity that formed between the applied force location and the new resistance location, which corresponded to the location of the outstanding leg of the angle since the connected leg was fractured. This eccentricity resulted in uncontrolled bending of the outstanding leg of the angle centred at the intersection of the fracture plane and the outstanding leg.

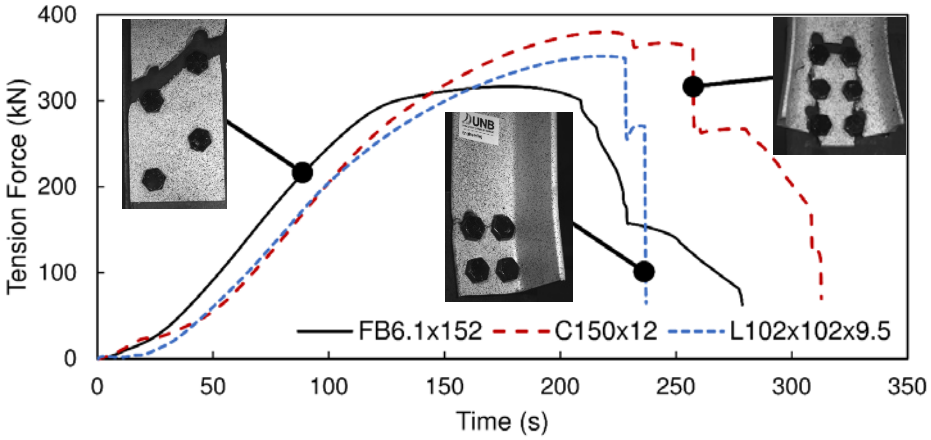

Figure 6: Applied tension load-time history for all three specimens

3 DIC VISUALIZATIONS OF FAILURES

Each of the specimens were analyzed using DIC to explore the strain behaviours at times corresponding to the onset of failure. The FB6.1x152 failure state, just prior to the first fracture occurring, is shown in Figure 7. Figure 7a shows the complete strain fields with both tension and compression strains visible. Here, the red region represents the high tension strain concentration around the inclined failure plane shown in Figure 7d. The tension only strains are shown in Figure 7b. This was achieved by modifying the scale of strains to display. In this case, the lower limit is set to zero strain and the upper limit set to 10% strain, a value far above yield. The tight grouping of strain contours that form along the fracture surface show the strain concentrations that correspond to necking at the onset of fracture. Figure 7c shows the compression strains only at the same load level as Figure 7a and b. Here, the bearing strains from the bolts onto the base material are shown in purple. It is of interest to note that all bolts produce similar compression strain fields in both magnitude and area, indicating a uniform distribution of the tension force into each bolt (ie, each bolt carries 1/4th the tension load in this connection).

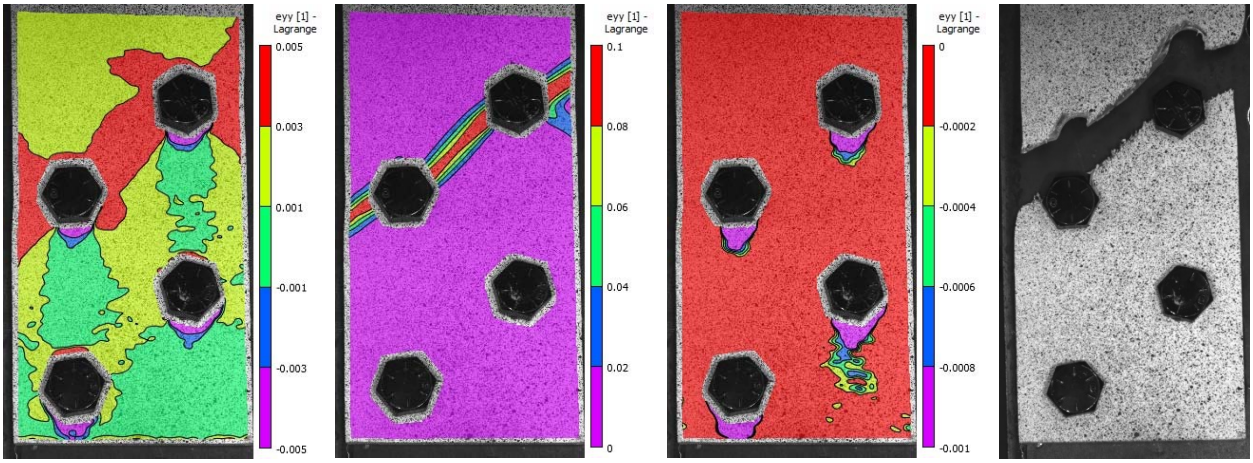

a) Full field longitudinal strains

b) Longitudinal tension strains

c) Longitudinal compression strains

d) Fractured specimen

Figure 7: Strain fields and failure mode of staggered bolt connection

The strain fields just prior to the tension and shear block failure on the bolted channel are shown in Figure 8a through e, while the failure block is shown in Figure 8f. Figure 8a shows the full longitudinal strain fields

in both tension and compression. In this figure, the tension strain concentrations around the leading bolts is evident and the high strain region between the bolts that comprises the tension component of the failure block is evident. Also evident in Figure 8a are the bearing strains shown in purple in the region behind the bolts themselves. Figure 8b highlights the tension strains by limiting the strains displayed to only positive (tension) values. Figure 8c shows the shear strains that are formed along the edges of the shear block. In this figure, the left and right shear strain concentrations are vey similar with a clear single shear plane following along the outside of each longitudinal line of fasteners to produce the shear block shown in Figure 8f. In Figure 8c, the strains on the left and right differ in sign, and therefore contour colour, due to a sign convention. Figure 8d shows the positive longitudinal strains with a different scale setting to cap the tension strain contours to approximately yield strain. In this figure, the very low strain values in the channel flange are evident and a rapid transition from high strain to low strain is visible at the web-flange interface. This figure clearly shows the shear lag present at the connection location where only the connected component contributes to resistance. Figure 8e shows the bearing strains from the bolts bearing directly on the base material by setting the displayed contours to only show negative (compression) longitudinal strains. Here it shows that all bolts contribute relatively equally to the force transfer in the section.

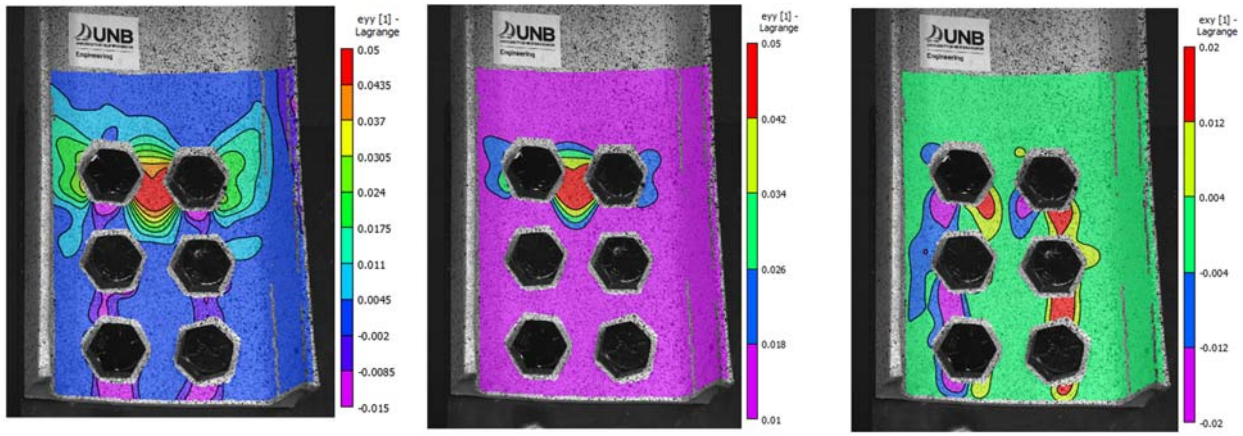

a) Full field longitudinal strains

b) Longitudinal tension strains

c) Shear Strains

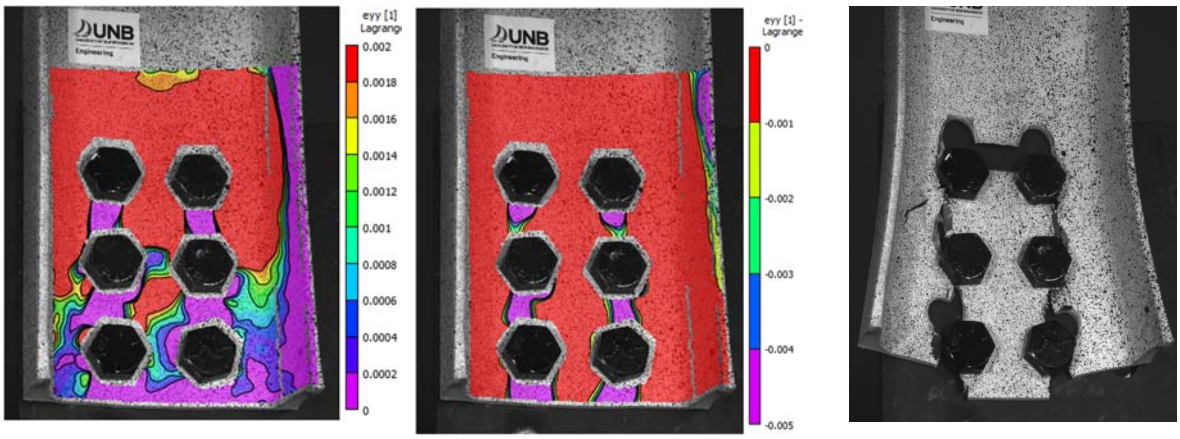

d) Longitudinal strains showing shear lag

e) Longitudinal compression strains

f) Fractured specimen

Figure 8: Strain fields at onset of failure of bolted channel connection

The strain fields and shear block failure mode for the L102x102x9.5 bolted angle are shown in Figure 9a through e, and the failed specimen is shown in Figure 9f. Figure 9 shows the full longitudinal strain field just prior to first rupture occurring in the specimen. Here, the high tension strain concentrations on the tension

failure plane on the asymmetrical block are clearly visible in red. The purple strains show the negative (compression) bearing strains due to bolt bearing. Figure 9b highlights the tension strain concentrations and shows the failure plane extending along the leading transverse line of bolts and extending to the free edge of the connected leg. A very small amount of strain concentrations extend into the unconnected outstanding leg. Figure 9c shows the shear strain concentrations that form along the longitudinal line of bolts closest to the outstanding leg, which forms the shear failure plane, making up part of the shear and tension failure block. Figure 9d is intended to show the shear lag phenomenon in this angle by limiting strain contours to only positive and capping them just under the yield strain value. There was a small amount of image correlation noise in this test that is especially evident in Figure 9d by the blotchy pattern on the outstanding leg. This noise is likely from glare or reflections from the light source causing low strain readings to be slightly variable, therefore, obscuring boundaries of contours for low magnitudes of strain. However, the presence of shear lag is still clearly identifiable by the low longitudinal strain values present in the outstanding leg when compared with the connected leg. Finally, Figure 9e shows the bearing strains from the bolts on the base material. Here, it is interesting to note the variability in bearing strains with the longitudinal line of bolts closest to the outstanding leg apparently carrying more of the tension force than the other two bolts. Additionally, the trailing bolt closest to the free edge of the connected leg carries almost none of the force in the connection. This asymmetric bolt demand is due to the relative stiffness of the member at different locations, with the bearing locations closest to the outstanding legs being far stiffer than the other locations and, therefore, being more inclined to attracting load once the specimen starts deforming as it approached ultimate capacity. This observation is critical to properly designing the number and size of bolts in such a connection.

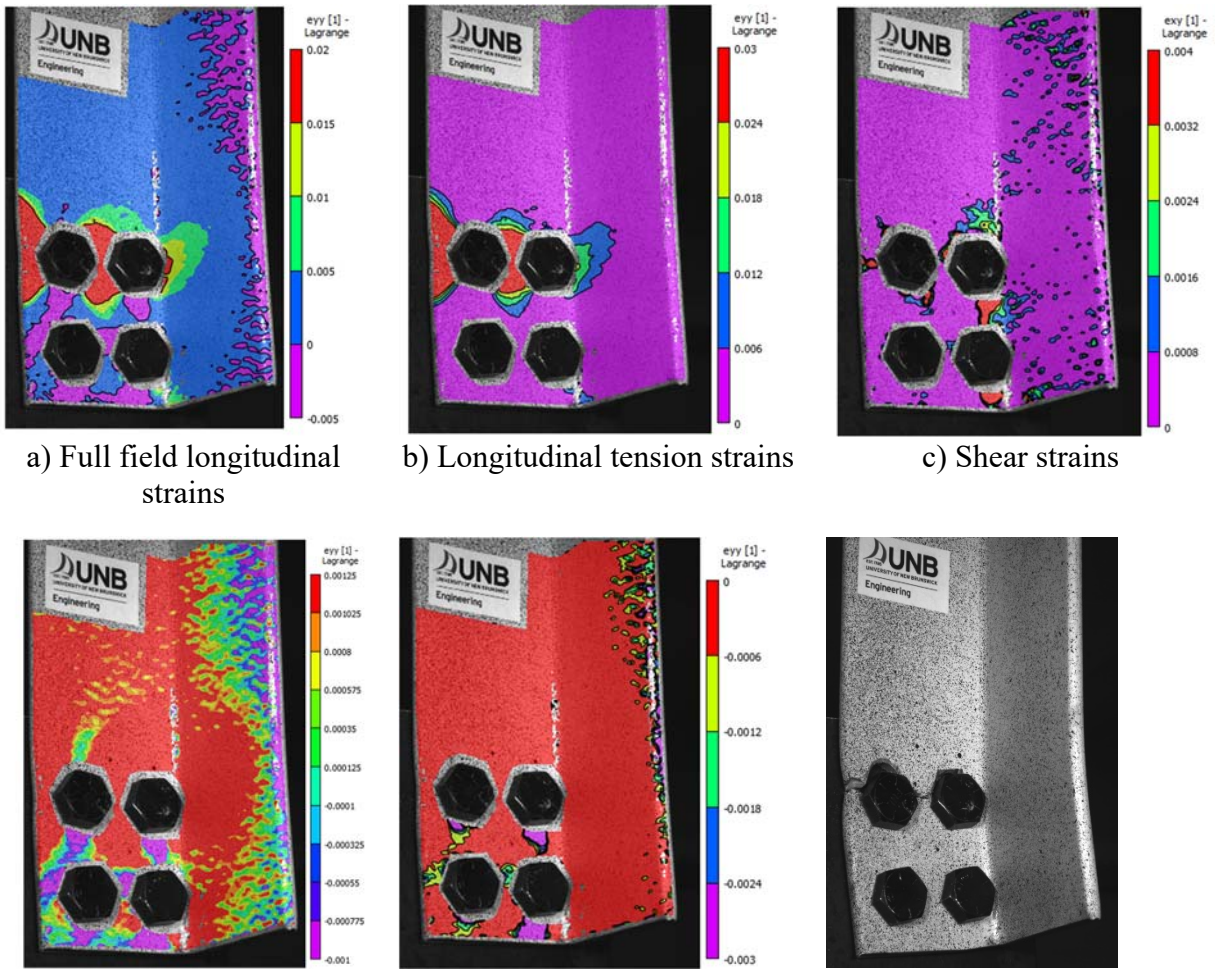

a) Full field longitudinal strains

b) Longitudinal tension strains

c) Shear strains

d) Longitudinal strains showing shear lag

e) Longitudinal compression strains

f) Fractured specimen

Figure 9: Strain fields at onset of failure of bolted angle connection

CSA S16-14 Design Equation Validation

The factored tension resistance (T_r) values along with the factored shear resistances of the bolt groups (V_r) and bearing resistances of the bolts bearing on the base metal (B_r) were computed using the measured material properties and are presented in Table 1.

Table 1: Summary of CSA S16-14 Design Resistance Values and Applied Load

Specimen	Material Properties		Eq [1]	Eq [2]	Eq [3]	Eq [4]	Eq [5]	Min Tension Resistance	Max Applied Load
	F_y (MPa)	F_u (MPa)	T_r (kN)	T_r (kN)	T_r (kN)	V_r (kN)	B_r (kN)	T_r (kN)	T (kN)
FB6.1x152	490	520	408.9	472.2	331.0	396.4	580.1	331.0	316.7
C150x12	390	510	544.1	576.5	364.4	594.7	1217	364.4	379.7
L102x102x9.5	375	500	624.4	244.8	328.5	396.4	868.7	244.8	351.8

The different tension, shear, and bearing resistance values in Table 1 were computed from equations in Cl. 13.2 (Equations 1 through 3 below) and Cl. 13.12.1.2 (Equations 4 and 5 below) of CSA S16-14.

[1] $T_r = \emptyset A_g F_y$

[2] $T_r = \emptyset_u \left[U_t A_n F_u + 0.6 A_{gv} \frac{(F_y + F_u)}{2} \right]$

[3] $T_r = \emptyset_u A_{ne} F_u$

[4] $V_r = 0.7 \times 0.6 \emptyset_b n m A_b F_u$

[5] $B_r = 3 \emptyset_{br} n t d F_u$

In Equation 4 above, the 0.7 factor accounts for the threads intercepting the shear planes for each connection.

The Minimum Tension Resistance for each member is shown in Table 1 alongside the Maximum Applied Load. This maximum applied load represents the actual ultimate capacity of the member, whereas the minimum tension resistance is the CSA S16-14 factored design resistance. Both the channel and the angle achieved conservative actual ultimate loads when compared against their design capacity. The flat bar failed at a load that was slightly lower than the factored design capacity, indicating a concerning unconservative design is present. However, all members had ultimate capacities similar to those given by the design equations. It should be noted that the factored design equations used material factors and actual measured material properties, so the capacity reducing material factors (ϕ=0.9, ϕ_u=0.75, ϕ_{br}=0.8) may be considered as overly conservative when comparing actual and design capacities.

The minimum tension resistance mode for the flat bar (Equation 3) and the angle (Equation 2) matched with the observed failure modes of inclined tension rupture and tension and shear block respectively. The minimum tension resistance mode for the channel (Equation 3) is governed by shear lag, whereas the channel clearly exhibited a tension and shear block at ultimate load. However, significant shear lag was present in the channel and shear lag does not produce an independent failure mode (ie, it promotes a different rupture mode by concentrating stresses on elements), so there is not necessarily a contradiction in the results. It appears that the shear lag along with the presence of the stiffening channel flanges near the shear planes in the tension and shear block contributed to an earlier tension and shear block failure than what is predicted in Equation 2 and that the shear lag design equation (Equation 3) did a good job in computing the design capacity of the channel.

4 CONCLUSIONS

The use of digital image correlation has allowed for a direct visualization of the failure modes for structural steel tension members and connections. These modes include yielding, rupture, tension and shear block, and shear lag. The structural elements tested in this study had capacities that were well predicted by CSA S16-14 Design of Steel Structures with one slightly unconservative result for the flat bar with staggered

bolts. The combination of the test data from the DIC, the applied force data, and the images of the failure modes create a tool for teaching tension member and connection design to university engineering students learning structural steel design concepts.

Acknowledgements

The authors would like to thank the University of New Brunswick Teaching and Learning Priority Fund program along with the University of New Brunswick Summer Employment Program for funding this project. Most steel material for this project was donated by OSCO Construction Group. Assistance in the laboratories from Andrew Sutherland and Chris Forbes was greatly appreciated.

The authors would like to make data and visualizations from this study, including but not limited to those contained here, available to interested steel educators. Interested parties may contact the corresponding author for details.

References

ASTM. 2015. Standard Specifications of High Strength Structural Bolts, Steel and Alloy Steel, Heat Treated, 120 ksi and 150 ksi Minimum Tensile Strength, Inch and Metric Dimensions. Standard ASTM F3125/3125M 15a, West Conshohocken, PA.

CSA. 2014. Limit states design of steel structures. Standard CAN/CSA-S16-14, Canadian Standards Association, Toronto, Ont.

McCormick, N. and Lord, J. 2010. Digital Image Correlation. *Materials Today*, **13**(12): 52-54.

SAE. 2011. Mechanical and Material Requirements for Externally Threaded Fasteners. Standard SAE J429, Warrendale, PA.